

Comparative Preclinical Pharmacokinetic and Metabolic Studies of the Combretastatin Prodrugs Combretastatin A4 Phosphate and A1 Phosphate

Ian G. Kirwan,^{1,2} Paul M. Loadman,¹
David J. Swaine,¹ D. Alan Anthoney,^{1,2}
George R. Pettit,³ John W. Lippert III,³
Steve D. Shnyder,¹ Patricia A. Cooper,¹ and
Mike C. Bibby¹

¹Cancer Research Unit, Tom Connors Cancer Research Centre, University of Bradford, Bradford, United Kingdom; ²Cancer Research United Kingdom Clinical Centre, St. James Hospital, University of Leeds, Leeds, United Kingdom; and ³Cancer Research Institute and Department of Chemistry, Arizona State University, Tempe, Arizona

ABSTRACT

Purpose: Combretastatin A4 phosphate (CA4P) and its structural analog, combretastatin A1 phosphate (CA1P), are soluble prodrugs capable of interacting with tubulin and causing rapid vascular shutdown within tumors. CA4P has completed Phase I clinical trials, but recent preclinical studies have shown that CA1P displays a greater antitumor effect than the combretastatin A4 (CA4) analog at equal doses. The aim of this study, therefore, is to compare pharmacokinetics and metabolism of the two compounds to determine whether pharmacokinetics plays a role in their differential activity.

Experimental Design: NMRI mice bearing MAC29 tumors received injection with either CA4P or CA1P at a therapeutic dose of 150 mg·kg⁻¹, and profiles of both compounds and their metabolites analyzed by a sensitive and specific liquid chromatography/mass spectroscopy method.

Results: The metabolic profile of both compounds is complex, with up to 14 metabolites being detected for combretastatin A1 (CA1) in the plasma. Many of these metabolites have been identified by liquid chromatography/mass spectroscopy. Initial studies, however, focused on the active components CA4 and CA1, where plasma and tumor areas under the curve were 18.4 and 60.1 μg·h·ml⁻¹ for CA4, and 10.4 and 13.1 μg·h·ml⁻¹ for CA1, respectively. *In vitro* metabolic comparisons of the two compounds strongly suggest

that CA1 is metabolized to a more reactive species than the CA4.

Conclusions: Although *in vitro* studies suggest that variable rates of tumor-specific prodrug dephosphorylation may explain these differences in pharmacokinetics profiles, the improved antitumor activity and altered pharmacokinetic profile of CA1 may be due to the formation of a more reactive metabolite.

INTRODUCTION

The combretastatins are a family of natural products derived from the African tree *Combretum caffrum* (1, 2) that have been shown to interact with tubulin (3) and cause vascular shutdown in solid tumors. They are structurally related to colchicine, another tubulin-binding agent, and contain two phenyl rings linked by a two-carbon bridge (Ref. 4; Fig. 1). These compounds are thought to function by binding tubulin at or near the colchicine-binding site, inhibiting assembly and ultimately resulting in the disruption of microtubular function (5). Treatment with combretastatin A4 (CA4), and its more soluble prodrug, combretastatin A4 phosphate (CA4P; Ref. 6), results in a reduction in blood flow within the tumor and subsequent massive hemorrhagic necrosis (7, 8). These results have been demonstrated at doses less than one-tenth of the maximum tolerated dose (7), offering a wide therapeutic window. In Phase I clinical trials in the United Kingdom and the United States, CA4P appears to be well tolerated, with some patients experiencing disease stability (9, 10) and a significant reduction in blood flow (11).

However, despite the potent antivasular effects of CA4P in tumors, CA4P induces little growth retardation when administered in single doses close to or at its maximum tolerated dose. This lack of activity has been attributed to the survival of a narrow rim of peripheral tumor cells adjacent to the more normal vasculature in the surrounding tissue (12). Such a viable region of cells is capable of rapid proliferation and contributes to the eventual regrowth and revascularization of the necrotic tumor center, although the cells would still be highly sensitive to additional chemotherapy (12–15).

Combretastatin A1 phosphate (CA1P; Ref. 4; Fig. 1) is a recently synthesized water-soluble prodrug of combretastatin A1 (CA1) with similar antitubulin properties to CA4P (1).

Recent studies have shown that CA1P has *in vivo* antitumor activity against a transplantable murine colon tumor, and this activity is also accompanied by severe hemorrhagic necrosis in the tumor (16). This new compound was tolerated up to a dose of 500 mg·kg⁻¹ and was more effective at producing tumor growth delay than CA4P (16, 17). These increased antitumor effects include a more efficient killing of the viable rim that remains after solid tumor treatment with CA4P. CA1P is also seen to be more efficacious against metastatic liver deposits of

Received 7/29/03; revised 11/5/03; accepted 11/7/03.

Grant support: The work of the Cancer Research Unit in Bradford is supported by Cancer Research United Kingdom Grant C459/A2579. The costs of publication of this article were defrayed in part by the payment of page charges. This article must therefore be hereby marked *advertisement* in accordance with 18 U.S.C. Section 1734 solely to indicate this fact.

Requests for reprints: Paul Loadman, Cancer Research Unit, University of Bradford, Bradford BD7 1DP, United Kingdom. Phone: 01274-233226; Fax: 01274-233234; E-mail: P.M.Loadman@Bradford.ac.uk.

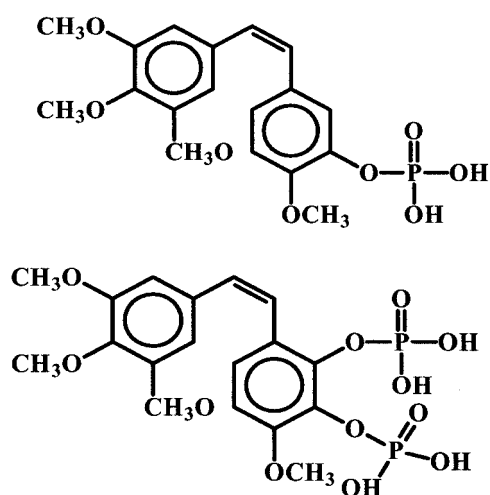


Fig. 1 Structural representation of prodrugs for combretastatin A4 (top) and combretastatin A1 (bottom).

HT-29 and DLD-1 colon tumors (18). Consequently, this work has identified CA1P as a preclinical developmental candidate with more potent antivasular and antitumor effects than CA4P when used as a single agent.

Although CA1P is a close analog of CA4, the extra hydroxyl group present on the second phenyl ring is clearly influential in the antitumor activity of the compound. The prodrugs, CA4P and CA1P (4, 6), were designed to be dephosphorylated *in vivo* via nonspecific phosphatases into active compounds (CA4 and CA1, respectively) and then transported intracellularly (5, 19). Therefore, it is quite possible that this extra phosphate group of the CA1P is influencing the pharmacokinetics, distribution, and release profile of the active compound CA1. For this reason, we investigated the pharmacokinetic profiles of prodrugs CA4P and CA1P in MAC29 tumor-bearing mice to determine whether pharmacokinetics plays a role in the differential activity of the two compounds. This work is also supported by *in vitro* studies investigating the rate of prodrug dephosphorylation and metabolism of the two compounds.

MATERIALS AND METHODS

Chemicals. CA1P and CA4P were synthesized at Arizona State University. The prodrugs were dissolved in saline immediately before use and protected from light at all times. All chemicals used for chromatography and mass spectroscopy were of high-performance liquid chromatography grade and purchased from Fisher Scientific Ltd. (Loughborough, United Kingdom).

Chromatography. The samples were analyzed by high performance liquid chromatography using a gradient system [mobile phase A = 90% 10 mM ammonium formate (pH 6.5), 10% methanol; mobile phase B = 35% 10 mM ammonium formate (pH 6.5), 65% methanol]. This mobile phase was used to develop a gradient in which mobile phase A contained 10% methanol, and mobile phase B contained 65%. The gradient was run initially at 50% B but increased to 95% over 25 min and was maintained for an additional 10 min. A Hichrom RPB (25 cm ×

4.6-mm; Hichrom Ltd., Reading, United Kingdom) column was used with a flow rate of 1.1 ml·min⁻¹. The flow rate was maintained, and samples were injected using a Waters Alliance 2690 (Milford, MA) quaternary pump chromatography system. Detection was performed using a Waters 996 photodiode array detector (λ_{\max} = 290 and 320 nm), which was connected in series with the chromatographic system.

Mass Spectroscopy. Liquid chromatography/mass spectroscopy analysis was carried out using a Waters ZMD (Micro-mass, Manchester, United Kingdom) quadrupole mass spectrometer connected in series to the Waters 2690. The mass spectrometer was operated in positive ion electrospray mode with a voltage of +3.00 kV applied to the capillary. A solvent flow of 1.1 ml·min⁻¹ (split 1:10) with a nitrogen gas flow of 400 liters·h⁻¹ and a source temperature of 180°C was used to produce stable spray conditions. The cone voltage was set at 25 V, and this gave clear mass spectra from these samples. The mass spectra were continuously scanned from *m/z* 1000 to *m/z* 100 every 3.5 s throughout the entire high-performance liquid chromatography separation. Masslynx software was used to process the mass spectral data and produce both total ion chromatograms and single ion recording chromatograms for the separation.

Drug Extraction. Fifty- μ l samples of either plasma or tissue homogenate were deproteinized by adding 2 volumes of acetonitrile, followed by centrifugation at 10,000 × *g* for 5 min. The supernatant was dried in a rotary vacuum evaporator (protected from light), and the samples were resuspended in 50 μ l of mobile phase A. These were centrifuged at 10,000 × *g* for 5 min before injection onto the high-performance liquid chromatography system.

Calibration Curve. Standard concentrations of CA1P (0–10 μ g·ml⁻¹) and CA4P (0–1.0 μ g·ml⁻¹) in both drug-free plasma and tumor tissue were plotted as concentration *versus* peak area. These data were used to calculate the amount of compound present from the pharmacokinetic samples.

Animals. Pure strain female NMRI mice (6–8 weeks old; B and K Universal Ltd., Hull, United Kingdom) were used. All mice had access to food (CRM diet; SDS, Witham, United Kingdom) and water *ad libitum*. The animals were kept in cages in an air-conditioned room with alternating cycles of light and dark. United Kingdom Coordinating Committee on Cancer Research (UKCCCR) guidelines (20) for the welfare of the animals in experimental neoplasia were adhered to throughout the study.

Tumor System. MAC29, a moderately well-differentiated, mucin producing transplantable murine colon adenocarcinoma (21), was used. The tumor was excised from a donor animal, placed in sterile physiological saline containing antibiotics, and cut into small fragments of approximately 2 mm³. Under brief general anesthesia, a single fragment was implanted into the flank of each mouse using a trocar. Once the tumors could be measured accurately, the mice were allocated into groups of three by restricted randomization to keep group mean tumor size variation to a minimum. Drug administration commenced when tumors could be reliably measured by calipers (tumor size, approximately 4 × 5 mm). All drug solutions were administered as a single i.p. dose of 150 mg·kg⁻¹.

Pharmacokinetic Studies. After drug administration, blood and tumor samples were taken at various time points

between 0 and 4 h, with three animals used at each time point. Blood was taken via cardiac puncture under terminal anesthesia and collected in heparinized tubes and placed on ice. Plasma was separated immediately by centrifugation ($5000 \times g$ for 10 min at 4°C) and stored at -20°C . Tumors were excised, snap frozen immediately in liquid nitrogen, and stored at -80°C until required. Tumor samples were homogenized [1:4 (w/v)] in homogenizing buffer (0.02 M Tris-HCl, 0.125 M NaCl, and 1% Triton X-100) and extracted as described above. Concentrations of prodrugs and active compounds were calculated from respective calibration curves. Pharmacokinetic parameters were calculated using standard pharmacokinetic calculations.

In Vitro Studies. To assess the rate of dephosphorylation and metabolism of prodrugs (CA1P and CA4P) or active compounds (CA1 and CA4) in tumor homogenates (1:4), plasma, and whole blood, samples were spiked with either compound to give a final concentration of $10 \mu\text{g}\cdot\text{ml}^{-1}$ and incubated at 37°C . The drug was extracted as described previously at various time points.

In Vitro Chemosensitivity Studies. The chemosensitivity of SW620 human colon adenocarcinoma cells to CA1P and CA4P was assessed *in vitro* over time using a modified version of the 3-(4,5-dimethylthiazol-2-yl)-2,5-diphenyltetrazolium bromide assay (22). SW620 cell concentration was adjusted to 1×10^4 cells/ml RPMI 1640 supplemented with 10% FCS, 1 mM sodium pyruvate, and 1 mM L-glutamine (all from Sigma, Poole, United Kingdom). This solution (180 μl) was added to each well of a 96-well plate, and cells were incubated for 48 h under standard conditions (37°C in a humidified atmosphere containing 5% carbon dioxide). CA1P and CA4P were prepared from a 10 mM DMSO stock solution, diluted with RPMI 1640 to give the necessary concentration, and applied to the wells for the required exposure time (1 h, 3 h, 24 h, or continuous exposure over 96 h). After incubation under standard conditions for the required time, the drug solutions were removed from the wells, and the cells were washed three times with HBSS (Sigma) before the addition of 200 μl of fresh medium. Plates were then incubated for 4 days after initial drug addition under standard conditions. After 4 days, the plates were processed for the 3-(4,5-dimethylthiazol-2-yl)-2,5-diphenyltetrazolium bromide assay, and the absorbance of the resulting solution was measured at 550 nm on a microtiter plate spectrophotometer. Results were expressed in terms of percentage survival, taking the absorbance of control cultures to be 100% survival. Chemosensitivity was expressed in terms of IC_{50} values, *i.e.*, the concentration of compound required to kill 50% of the cell population.

RESULTS

Chromatography. Good separation of standards was achieved using the system described, with no endogenous substances found in drug-free plasma or tumor interfering with the major peaks of interest. The extraction efficiencies for CA1 and CA4, both phosphate prodrugs and active forms, were calculated from plasma and tumor compared with those in saline. All extraction efficiencies from both plasma and tumor were $>80\%$, and details are given in Table 1. Standards were also monitored using full photodiode array capability to monitor for *cis-trans* conversion. Such conversion could be induced naturally by

Table 1 Summary of the relative extraction efficiencies of CA1,^a CA1P, CA4, and CA4P from plasma and MAC 29 tumor samples ($n = 4 \pm 1$ SD)

	Matrix	Extraction efficiency (%)
CA4P	Tumor	99.3 \pm 0.34
CA4	Tumor	98.7 \pm 0.67
CA1P	Tumor	100.8 \pm 0.28
CA1	Tumor	101.9 \pm 1.13
CA4P	Plasma	98.6 \pm 3.91
CA4	Plasma	101.6 \pm 8.12
CA1P	Plasma	91.1 \pm 10.9
CA1	Plasma	90.8 \pm 4.24

^a CA1, combretastatin A1; CA1P, combretastatin A1 phosphate; CA4P, combretastatin A4 phosphate; CA4, combretastatin A4.

exposing the prodrug to light for several minutes and monitoring *cis* products at 280 nm and *trans* products at 330 nm.

Mass Spectroscopy. During the method validation, standards of CA1P, CA1, CA4P, and CA4 were scanned using liquid chromatography/mass spectroscopy, and parent ion single ion recording channels were established. All standards gave clear spectra using the liquid chromatography/mass spectroscopy system described.

By using such specific detection, single ion recording channels could be used to monitor selected compounds in what was a complex metabolic profile. Channels for the CA1 biphosphate (m/z 493.2), the CA1 monophosphate (m/z 413.2), the CA1 active product (m/z 333.3), CA4P (m/z 396.6), and CA4 (m/z 317.5) were established. From the chromatography results during isolation, it was clear that there were two potential monophosphate CA1 intermediates capable of forming from the biphosphate CA1 prodrug, each with identical spectra and mass.

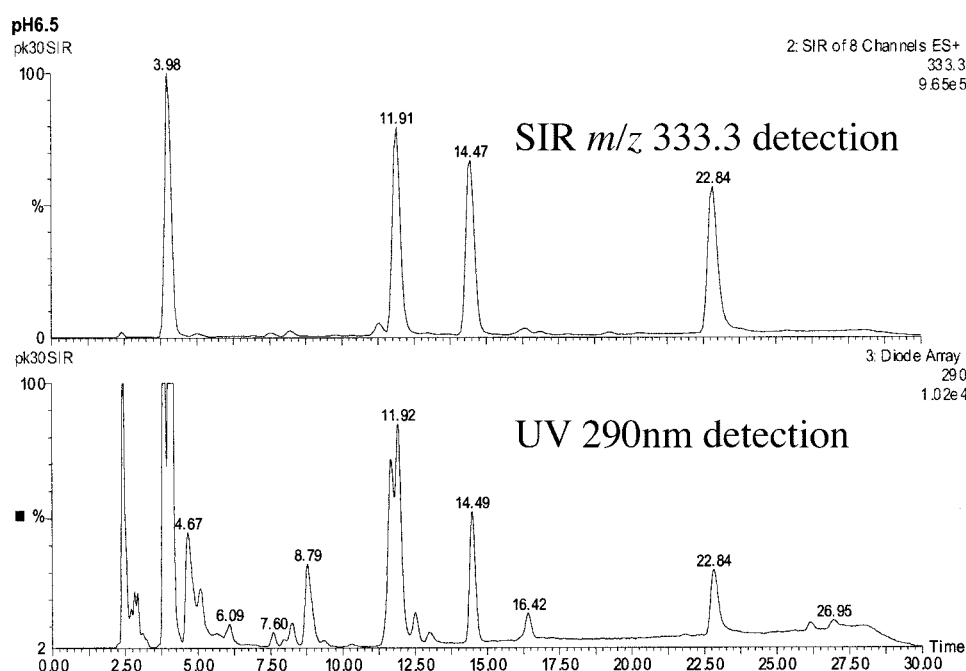
Calibration Curves. Calibration curves generated using absorption at 290 nm were prepared separately for CA1 prodrug, CA1, CA4P, and CA4. All curves were linear over the range tested, and reproducibility at the midpoint was $<15\%$.

Pharmacokinetic Studies. Pharmacokinetic samples from mice previously given CA1P at $150 \text{ mg}\cdot\text{kg}^{-1}$ *i.p.* gave a complex picture of prodrug metabolism in the plasma (Fig. 2), showing at least 13 metabolites of the parent prodrug. However this metabolic profile could be dissected in some detail with the use of electrospray mass spectroscopy, and many of the plasma metabolites have been proposed as glucuronides based on their polarity and mass ($M_r > 500$). These findings can be seen in more detail in Fig. 3. It is worthwhile to note that the peak at 8.8 min (Fig. 3, 8; m/z 329.4) may correspond to a potentially reactive *o*-quinone. A summary of the pharmacokinetic parameters for the main metabolites and intermediates is given in Table 2. The profile of active drug metabolism in the tumor was simpler than that observed in plasma (Fig. 4).

The plasma profile after administration of CA4P at $150 \text{ mg}\cdot\text{kg}^{-1}$ was not as complex as that with CA1P (Fig. 3), presumably due to the fact that a single phosphate on the prodrug does not allow the same number of metabolic options as the biphosphate CA1P.

Graphical representation of the disposition of either active CA1 or active CA4 clearly shows that concentrations of CA4 are higher than those of CA1 in both plasma and tumor (Fig. 5).

Fig. 2 Typical high performance liquid chromatography traces of plasma after i.p. administration of combretastatin A1 prodrug at 150 mg/kg show single ion recording (top; SIR) and UV detection at 290 nm (bottom).



Peak plasma concentrations for CA1 and CA4 are 16.4 and 43.2 $\mu\text{g}\cdot\text{ml}^{-1}$, respectively, with plasma areas under the curve (AUCs) being 10.4 $\mu\text{g}\cdot\text{h}\cdot\text{ml}^{-1}$ for CA1 and 18.4 $\mu\text{g}\cdot\text{h}\cdot\text{ml}^{-1}$ for CA4. Surprisingly, tumor concentrations of CA1, both peak concentrations and AUCs, were considerably lower for CA1 than those of CA4, with tumor AUC for CA1 (13.1 $\mu\text{g}\cdot\text{h}\cdot\text{ml}^{-1}$) being 4-fold lower than that for CA4 (60.1 $\mu\text{g}\cdot\text{h}\cdot\text{ml}^{-1}$). Although the presence of CA1 is underrepresented by the AUC value for active compound (due to unconverted phosphorylated prodrug), combining AUCs for all forms of active and prodrug still suggests lower concentrations of CA1 (27.1 $\mu\text{g}\cdot\text{h}\cdot\text{ml}^{-1}$) than CA4 (61.6 $\mu\text{g}\cdot\text{h}\cdot\text{ml}^{-1}$) in tumor.

Possibly because of the extra phosphate on the CA1 prodrug, active CA1 may not be released as rapidly as CA4. Several intermediates (Fig. 3) can be visualized, including two CA1P monophosphate peaks, which both appear to be in the *cis*-conformation, as well as previously mentioned glucuronides. Many of the CA1 intermediates are present even at 4 h after drug administration, which may account for the lower amounts of CA1 seen in the tumor. We have therefore monitored rates of dephosphorylation in various matrices to see whether this accounts for the varied distribution of active compound.

In Vitro Dephosphorylation Studies. These revealed that CA1P and CA4P were relatively stable in murine plasma, with little evidence of dephosphorylation even after 3 h. In blood, the prodrugs had broken down slightly more than in plasma, with the rate approaching 133 $\text{ng}\cdot\text{g}\cdot\text{min}^{-1}$ in the case of CA4P. As expected, however, the prodrugs were rapidly dephosphorylated in tumor (MAC29) and liver preparations, with rates in each case of >1000 $\text{ng}\cdot\text{g}\cdot\text{min}^{-1}$ (Table 3).

In Vitro Metabolism Analysis. Due to the lower overall tumor concentrations of the more potent CA1 and the complex plasma profile of CA1 and associated metabolites, we felt it

necessary to undertake preliminary *in vitro* metabolism studies in tumor homogenates. This was to investigate the potential of differential tumor metabolism between CA4 and CA1 and/or the formation of a highly potent metabolite within the tumor. Metabolic results from the active CA1 or CA4 incubated in MAC29 tumor homogenate at 37°C are presented graphically in Fig. 6, and although no metabolite formation was detected with either compound, the disappearance of CA1 compared with CA4 was remarkably rapid. This was a very reproducible effect, and the experiment was repeated on four independent occasions.

A comparative study, using colchicine (data not shown), was also set up to establish how the metabolism of this classical tubulin binder compared with that of the combretastatins. Results indicated that colchicine was actually more stable than either combretastatin, with 100% recovery after a 4-h extraction.

IC₅₀ 3-(4,5-Dimethylthiazol-2-yl)-2,5-diphenyltetrazolium Bromide Assay. Because there was clearly a differential in metabolic rates between the two combretastatins, we revisited the *in vitro* cytotoxicity assays. Because MAC29 is not available as a cell line, cytotoxicity data were assessed using SW620 cells. Long-term exposures (96 and 24 h) to active drug revealed that both CA1 and CA4 had similar IC₅₀ values (Table 4). Assays carried out at 1- and 3-h exposures revealed that CA1 was more effective in killing the host cells, with IC₅₀ values for CA1 up to three times lower than those for CA4 in the 1-h assay.

DISCUSSION

Although CA4 is known to be an efficient tubulin binder (2, 3) causing vascular shutdown and tumor necrosis, previous evidence suggests that CA1 is more active in both *s.c.* and clinically relevant tumor models (18). The aim of this study,

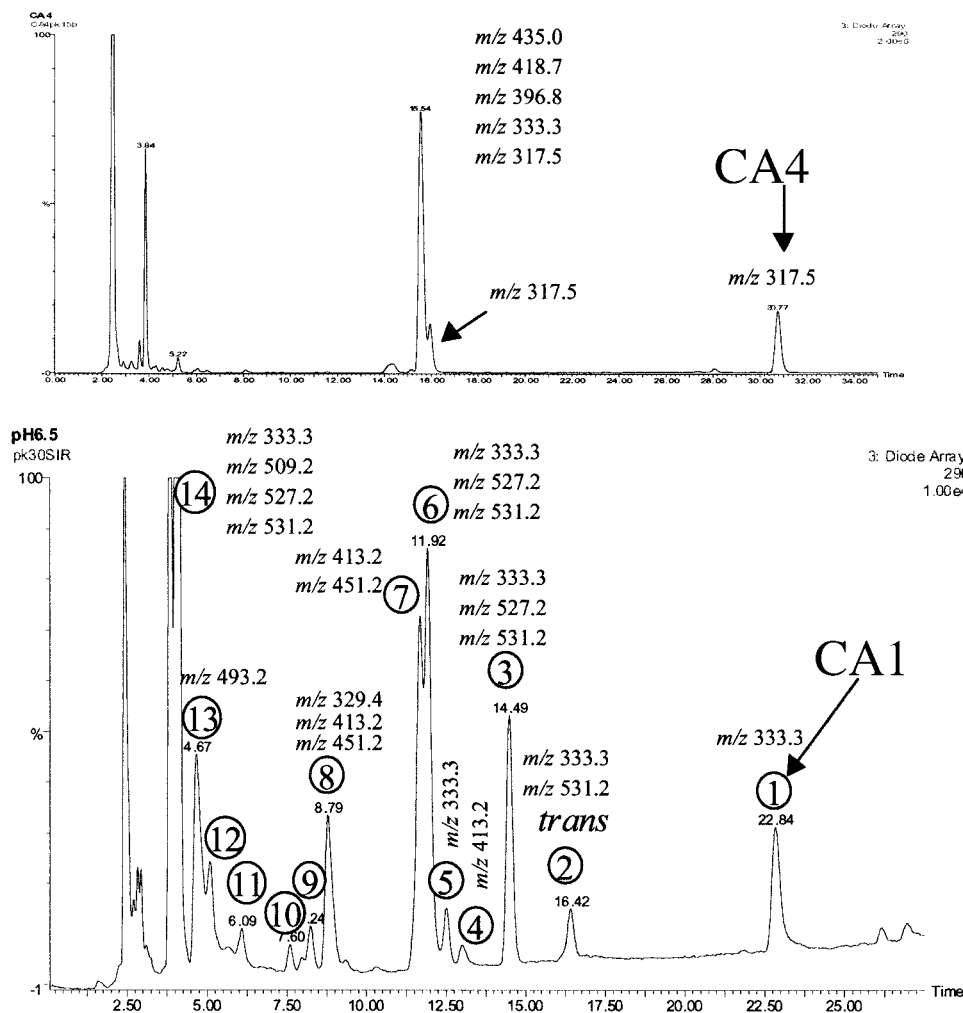


Fig. 3 Typical high performance liquid chromatography trace at 290 nm (also showing related MS data) of combretastatin A4 (top) and combretastatin A1 (bottom) with related metabolites in plasma 15 (combretastatin A4) and 30 min (combretastatin A1) after administration of prodrug at 150 mg/kg i.p. Combretastatin A1 (1) is highlighted with at least 13 metabolites.

therefore, was to investigate whether there was a pharmacokinetic component to this differential activity.

The analytical methods that have been developed were highly specific and sensitive and were very reproducible. Therefore, it was surprising that tumor concentrations of active CA1 ($C_{\max} = 11 \mu\text{g}\cdot\text{ml}^{-1}$, $\text{AUC} = 13 \mu\text{g}\cdot\text{h}\cdot\text{ml}^{-1}$) were approxi-

mately 4-fold lower than those detected for CA4 ($C_{\max} = 37 \mu\text{g}\cdot\text{ml}^{-1}$, $\text{AUC} = 60 \mu\text{g}\cdot\text{h}\cdot\text{ml}^{-1}$), whereas plasma concentrations were approximately the same. The slight differential seen in plasma concentrations can be explained by the complex profile of metabolites seen after administration of the CA1 prodrug. Many of these metabolites can be accounted for by

Table 2 Pharmacokinetic data summary for CA4P^a and CA1P including dephosphorylated metabolites in plasma and tumor after i.p. administration of the prodrug at 150 mg/kg

		T_{\max} (min)	C_{\max} ($\mu\text{g}\cdot\text{ml}^{-1}$)	$t_{1/2}$ (h)	$\text{AUC}_{0-4\text{h}}$ ($\mu\text{g}\cdot\text{h}\cdot\text{ml}^{-1}$)
CA1	Plasma	15	16.4	9.02	10.4
	Tumor	15	11.0	3.31	13.1
CA1MP	Plasma	15	67.6	5.87	43.7
	Tumor	15	6.07	1.47	6.67
CA1P	Plasma	N/D	N/D	N/D	
	Tumor	15	6.83	2.41	7.31
CA4	Plasma	15	43.2	0.35	18.4
	Tumor	30	36.8	9.62	60.1
CA4P	Plasma	15	95.2	1.38	40.6
	Tumor	30	1.32	0.72	1.52

^a CA1, combretastatin A1; CA1MP, combretastatin A1 mono phosphate; CA1P, combretastatin A1 phosphate (prodrug); CA4, combretastatin A4; CA4P, combretastatin A4 phosphate.

Fig. 4 Typical high performance liquid chromatography traces of tumor (MAC29) extract 15 min after i.p. administration of prodrug at 150 mg/kg.

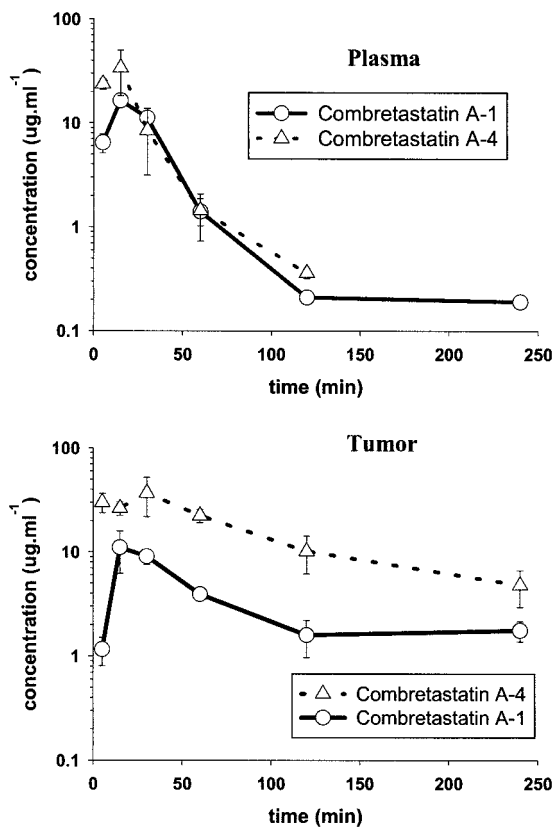
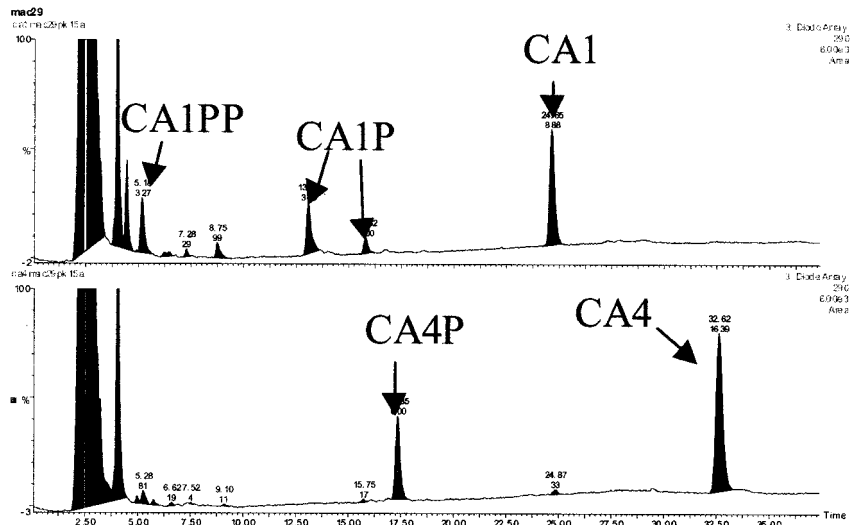


Fig. 5 Concentrations of active combretastatin A1 (○, solid line) or A4 (△, dotted line) in plasma (top) or tumor (bottom) after i.p. administration of prodrug at 150 mg/kg.

CA1 compared with CA4. This fact still does not account for the increased efficacy of CA1 over CA4 because lower concentrations of CA1 were detected in tumor. Dephosphorylation studies may explain the pharmacokinetic differences between the two

Table 3 Dephosphorylation rates of combretastatin A1 phosphate and combretastatin A4 phosphate in blood, plasma, liver, and MAC29 tumors

Tissue	Rates (ng/g/min)	
	CA1P ^a	CA4P
Plasma	~30	~30
Blood	~30	133
Tumor (MAC29)	>1000	>1000
Liver	>1000	>1000

^a CA1P, combretastatin A1; CA4P, combretastatin A4.

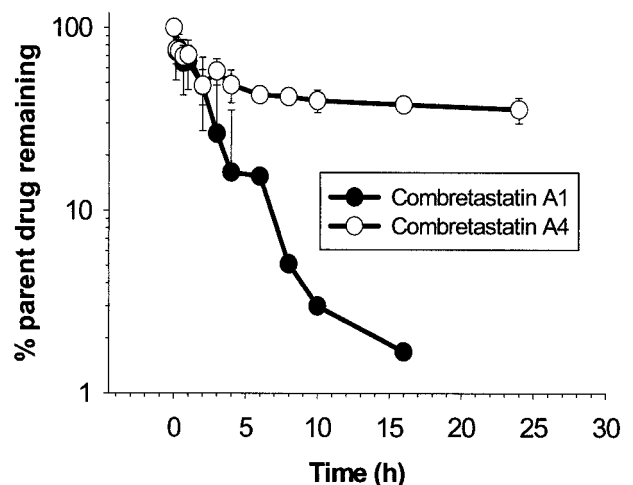


Fig. 6 Metabolism of active combretastatin A1 (●) and combretastatin A4 (○) in MAC29 tumor homogenate (values are from four independent experiments).

both the intermediate monophosphates and glucuronides of the active CA1. Clearly, the additional phosphate on the CA1 (or the additional hydroxyl group to which the phosphate is attached) does influence both the metabolism and disposition of

Table 4 *In vitro* IC₅₀ data showing the cytotoxicity of CA1^a and CA4 on host SW620 cells

Time of exposure (h)	IC ₅₀ (nM)	
	CA1	CA4
96	0.36	0.38
24	2.10	2.90
3	12.00	32.00
1	11.00	36.00

^a CA1, combretastatin A1; CA4, combretastatin A4.

compounds because in whole blood, CA4P was clearly dephosphorylated faster than CA1P, although both liver and tumor showed such a rapid degradation of prodrug to active species that we did not feel it necessary to differentiate between the rates for CA1 and CA4.

Although tumor profiles of both compounds were not as complex as those for plasma, we initiated additional *in vitro* metabolic studies on the active CA1 and CA4 in the responsive MAC29 tumor homogenates, using the selective and sensitive liquid chromatography/mass spectroscopy system. We were searching for tumor-specific cytotoxic metabolites generated from the more efficacious CA1 and not the less active CA4, which may have explained the enhanced activity. It was therefore unexpected when no metabolites were detected, but parent compound concentration decreased. CA1 disappeared rapidly after a 2-h lag phase, whereas CA4 was relatively stable and was still detectable after 24 h of incubation. Colchicine was introduced into the study for comparison and found to be more stable than both CA1 and CA4, with close to 100% remaining after 4 h. This disappearance of parent compound is suggestive of covalently bound drug because the extraction process was relatively aggressive and very reproducible.

It was reported previously that CA4 and CA1 had equivalent activities as inhibitors of tubulin polymerization, whereas CA1 appeared to be somewhat more active as an inhibitor of the binding of colchicine to tubulin (2, 23). On studying the binding of drug to isolated tubulin in the analytical system described over 24 h, close to 100% of drug was recovered,⁴ suggesting that tubulin itself may not be the cause of the rapid disappearance of CA1.

Considering that there is an initial lag period of 2 h for the CA1 to start diminishing along with CA4 (see Fig. 6), this could well be due to a possible threshold time for effective binding to take place. Thus, it was important to revisit the *in vitro* cytotoxicity studies to confirm that both compounds were of equal potency. These studies confirmed that both combretastatins are very potent cytotoxic agents with IC₅₀ values in the picomolar range after continuous exposure. These values confirm previous studies (23), and short-term exposures investigated in this study over a 1-h time period are proportionately higher but still in the low nanomolar range [11 nM (3.3 ng·ml⁻¹) for CA1]. When using these shorter exposure parameters, differences can be seen between CA1 and CA4, with the IC₅₀ for the former being three

times lower after a 1-h exposure. Although these IC₅₀ values are so low for the active CA1 *in vitro*, calculated pharmacokinetic parameters clearly show that peak drug concentrations in tumor ($C_{\max} = 11,000 \text{ ng}\cdot\text{ml}^{-1}$) are approximately 3000 times this value, and with maximum tolerated doses in mice in excess of 200 mg·kg⁻¹, the compound is clearly not toxic *in vivo*. This is a property of these compounds that must be investigated in future studies.

In conclusion, this study has shown that pharmacokinetic profiles of the CA1 and CA4 are unlikely to explain the differential antitumor activity seen *in vivo*. Although plasma profiles of the active components were similar, 4-fold less CA1 was detected in the tumor than CA4. There were marked differences, however, in *in vitro* metabolism between the two compounds that may explain the decreased tumor concentrations of CA1. The formation of a reactive CA1 metabolite cannot be ruled out, and indeed, now it seems very likely that such an active metabolite might arise by *in vivo* conversion of CA1P to a very reactive *o*-quinone. The *o*-quinone would be derived from the vicinal diphenol created by a reaction cascade after dephosphorylation. We are now pursuing such a potentially reactive metabolite.

REFERENCES

- Pettit, G. R., Singh, S. B., Niven, M. L., Hamel, E., and Schmidt, J. M. Antineoplastic agents 124. Isolation, structure, and synthesis of combretastatin-a-1 and combretastatin-B-1, potent new inhibitors of microtubule assembly, derived from *Combretum caffrum*. *J. Natural Products*, 50: 119–131, 1987.
- Pettit, G. R., Singh, S. B., Hamel, E., Lin, C. M., Alberts, D. S., and Garciakendall, D. Antineoplastic agents 145. Isolation and structure of the strong cell-growth and tubulin inhibitor combretastatin-a-4. *Experientia (Basel)*, 45: 209–211, 1989.
- Lin, C. M., Singh, S. B., Chu, P. S., Dempsy, R. O., Schmidt, J. M., Pettit, G. R., *et al.* Interactions of tubulin with potent natural and synthetic analogs of the antimetabolic agent combretastatin: a structure-activity study. *Mol. Pharmacol.*, 34: 200–208, 1988.
- Pettit, G. R., and Lippert, J. W. Antineoplastic agents 429. Syntheses of the combretastatin A-1 and combretastatin B-1 prodrugs. *Anti-Cancer Drug Des.*, 15: 203–216, 2000.
- McGown, A. T., and Fox, B. W. Structural and biochemical-comparison of the anti-mitotic agents colchicine, combretastatin-A4 and amphetamine. *Anti-Cancer Drug Des.*, 3: 249–254, 1989.
- Pettit, G. R., Temple, C., Narayanan, V. L., Varma, R., Simpson, M. J., Boyd, M. R., *et al.* Antineoplastic agents 322. Synthesis of combretastatin A-4 prodrugs. *Anti-Cancer Drug Des.*, 10: 299–309, 1995.
- Dark, G. G., Hill, S. A., Prise, V. E., Tozer, G. M., Pettit, G. R., and Chaplin, D. J. Combretastatin A-4, an agent that displays potent and selective toxicity toward tumor vasculature. *Cancer Res.*, 57: 1829–1834, 1997.
- Grosios, K., Holwell, S. E., McGown, A. T., Pettit, G. R., and Bibby, M. C. *In vivo* and *in vitro* evaluation of combretastatin A-4 and its sodium phosphate prodrug. *Br. J. Cancer*, 81: 1318–1327, 1999.
- Dowlati, A., Robertson, K., Cooney, M., Petros, W. P., Stratford, M., Jesberger, J., *et al.* A Phase I pharmacokinetic and translational study of the novel vascular targeting agent combretastatin A-4 phosphate on a single-dose intravenous schedule in patients with advanced cancer. *Cancer Res.*, 62: 3408–3416, 2002.
- Remick, S., Robertson, K., Dowlati, A., Cooney, M., Jesberger, J., Lewin, J., *et al.* A Phase I pharmacokinetic (PK) study of single dose intravenous (IV) combretastatin A4 phosphate (CA4P) in patients (PTS)

⁴ I. G. Kirwan and P. M. Loadman, unpublished data.

- with advanced cancer: final report. *Clin. Cancer Res.*, 7 (Suppl.): 393, 2001.
11. Galbraith, S. M., Taylor, N. J., Maxwell, R. J., Lodge, M., Tozer, G. M., Baddeley, H., *et al.* Combretastatin A4 phosphate (CA4P) targets vasculature in animal and human tumours. *Br. J. Cancer*, 83 (Suppl. 1): 12, 2000.
 12. Chaplin, D. J., Pettit, G. R., and Hill, S. A. Anti-vascular approaches to solid tumour therapy: evaluation of combretastatin A4 phosphate. *Anticancer Res.*, 19: 189–195, 1999.
 13. Grosios, K., Loadman, P. M., Swaine, D. J., Pettit, G. R., and Bibby, M. C. Combination chemotherapy with combretastatin A-4 phosphate and 5-fluorouracil in an experimental murine colon adenocarcinoma. *Anticancer Res.*, 20: 229–233, 2000.
 14. Murata, R., Siemann, D. W., Overgaard, J., and Horsman, M. R. Interaction between combretastatin A-4 disodium phosphate and radiation in murine tumors. *Radiother. Oncol.*, 60: 155–161, 2001.
 15. Nelkin, B. D., and Ball, D. W. Combretastatin A-4 and doxorubicin combination treatment is effective in a preclinical model of human medullary thyroid carcinoma. *Oncol. Rep.*, 8: 157–160, 2001.
 16. Holwell, S. E., Cooper, P. A., Grosios, K., Lippert, J. W., Pettit, G. R., Shnyder, S. D., *et al.* Combretastatin A-1 phosphate a novel tubulin-binding agent with *in vivo* antivascular effects in experimental tumours. *Anticancer Res.*, 22: 707–711, 2002.
 17. Hill, S. A., Tozer, G. M., Pettit, G. R., and Chaplin, D. J. Preclinical evaluation of the antitumour activity of the novel vascular targeting agent oxi 4503. *Anticancer Res.*, 22: 1453–1458, 2002.
 18. Holwell, S. E., Cooper, P. A., Thompson, M. J., Pettit, G. R., Lippert, J. W., Martin, S. W., *et al.* Anti-tumor and anti-vascular effects of the novel tubulin-binding agent combretastatin A-1 phosphate. *Anticancer Res.*, 22: 3933–3940, 2002.
 19. Pettit, G. R., and Rhodes, M. R. Antineoplastic agents 389. New syntheses of the combretastatin A-4 prodrug. *Anti-Cancer Drug Des.*, 13: 183–191, 1998.
 20. UKCCCR Guidelines for the Welfare of Animals in Experimental Neoplasia. *Br. J. Cancer*, 77: 1–10, 1998.
 21. Double, J. A., Ball, C. R., and Cowen, P. N. Transplantation of adenocarcinomas of the colon in mice. *J. Natl. Cancer Inst. (Bethesda)*, 54: 271–275, 1975.
 22. Mosman, T. Rapid colorimetric assay for cellular growth and survival: application to proliferation and cytotoxicity assays. *J. Immunol. Methods*, 65: 55–63, 1983.
 23. Pettit, G. R., Lippert, J. W., Herald, D. L., Hamel, E., and Pettit, R. K. Antineoplastic agents 440. Asymmetric synthesis and evaluation of the combretastatin A-1 SAR probes (1*S*,2*S*)- and (1*R*,2*R*)-1,2-dihydroxy-1-(2',3'-dihydroxy-4'-methoxyphenyl)-2-(3'',4'',5''-trimethoxyphenyl)-ethane. *J. Natural Products*, 63: 969–974, 2000.

Clinical Cancer Research

Comparative Preclinical Pharmacokinetic and Metabolic Studies of the Combretastatin Prodrugs Combretastatin A4 Phosphate and A1 Phosphate

Ian G. Kirwan, Paul M. Loadman, David J. Swaine, et al.

Clin Cancer Res 2004;10:1446-1453.

Updated version Access the most recent version of this article at:
<http://clincancerres.aacrjournals.org/content/10/4/1446>

Cited articles This article cites 23 articles, 3 of which you can access for free at:
<http://clincancerres.aacrjournals.org/content/10/4/1446.full#ref-list-1>

Citing articles This article has been cited by 6 HighWire-hosted articles. Access the articles at:
<http://clincancerres.aacrjournals.org/content/10/4/1446.full#related-urls>

E-mail alerts [Sign up to receive free email-alerts](#) related to this article or journal.

Reprints and Subscriptions To order reprints of this article or to subscribe to the journal, contact the AACR Publications Department at pubs@aacr.org.

Permissions To request permission to re-use all or part of this article, use this link
<http://clincancerres.aacrjournals.org/content/10/4/1446>.
Click on "Request Permissions" which will take you to the Copyright Clearance Center's (CCC) Rightslink site.